

See discussions, stats, and author profiles for this publication at: <http://www.researchgate.net/publication/224163324>

Design of a Model-Scale Air-Core Compulsator

ARTICLE *in* IEEE TRANSACTIONS ON PLASMA SCIENCE · FEBRUARY 2011

Impact Factor: 1.1 · DOI: 10.1109/TPS.2010.2053221 · Source: IEEE Xplore

CITATIONS

2

READS

238

5 AUTHORS, INCLUDING:



[Qianfan Zhang](#)

Harbin Institute of Technology

29 PUBLICATIONS 107 CITATIONS

[SEE PROFILE](#)



[Shaopeng Wu](#)

Harbin Institute of Technology

22 PUBLICATIONS 20 CITATIONS

[SEE PROFILE](#)

Design of a Model-Scale Air-Core Compulsator

Qianfan Zhang, Shaopeng Wu, *Student Member, IEEE*, Chengda Yu, Shumei Cui, and Liwei Song

Abstract—A preliminary design scheme of a model-scale compulsator, which is the heart of the railgun pulse-power system, is provided in this paper. The model-scale air-core compulsator, which can provide considerable energy, power density, and energy density, is the best choice for pulse-power supply of a railgun system equipped to an amphibious assault vehicle. To allow rapid sizing of compulsator systems, it is necessary to present the main first-stage design process which can be used to design systems for advanced applications. Three main aspects during the design of a model-scale compulsator are necessarily presented in this paper: the simulation and calculations of air-core electromagnetic field; the evaluation of extremely high forces imposed during the discharge; and the choice of cooling method of the windings due to the large level of armature current and excitation current. The topology of the model-scale compulsator is chosen. The compulsator has no concrete compensation component, and the excitation winding does the excitation and compensation simultaneously. The design of the model-scale is based on research of a small-scale air-core principle prototype. The feasibility of the technique and machining is also demonstrated. In addition, the main auxiliary components, such as the high-temperature superconducting magnetic bearing and the high-speed brush slip-ring mechanism, are discussed according to the operating conditions.

Index Terms—Air core, compulsator, model scale, railgun power supplies.

I. INTRODUCTION

COMPENSATED pulsed alternator (CPA), a type of inertia energy-storage technology, is a new kind of pulsed-power based on the armature-reaction compensation and magnetic-flux compression. The pulse-power technology has broad prospects in many high-tech fields, such as electromagnetic launch, directed energy weapon, and so on.

As a power source for electric guns, CPA has been under development for many years [1]–[5] with a wide range of configurations, including rotating armature, rotating field, iron core, air core, externally excited, and self-excited. With the transition from iron-core to air-core magnetic circuits and the associated incorporation of composite materials and self-excitation, the energy density and power density have obtained substantial increases. The energy density increased from 4 to 14.4 J/g, from the iron-core compulsator to the model-scale

compulsator. The power density increased from 0.1 kW/g of iron-core compulsator to 2.1 kW/g of the model-scale compulsator. Although the increase in energy density and power density is remarkable, it cannot satisfy the requirement of pulsed-power supply for equipping mobile combat vehicle and fighter in practice.

Due to the complex nature of compulsator design and optimization, a relatively simple and straightforward design process is critically needed to support the evaluation at an overall system level before an engineering prototype is fabricated. The model-scale compulsator is different from the traditional large-level electrical machine. First, the topology should be chosen for obtaining higher energy density and power density. Second, the evaluation of electromagnetic field, mechanical stress, and thermal-heat aspects are decided by the nature of pulsed operation. Finally, the selection of main auxiliary component and technique and machining of composite rotor and slotless winding are discussed.

II. CHOICE OF TOPOLOGY

The CPA is a synchronous generator intentionally designed to maximize short-circuit-current output by minimizing internal impedance through the action of flux compression and/or air-core topology. Flux compression is achieved through the use of special internal windings (compensating windings) normally referred to as one of three classes as passive, selective passive, or active. In some cases, there may be no compensating winding used, although the field winding mimics the function of a wound compensating winding itself and will compress the flux between itself and the armature for parts of the discharge cycle [6]. The design of the model-scale compulsator belongs to this case.

In order to achieve higher energy and power densities, the most influential factor is the choice of topologies. A detailed comparison of different topologies in terms of rotor energy density, EM coupling, electrical frequency, and discharge shear stress was made in [7]. Compared with the previous topologies, the preferred compulsator topology is a modified rim rotor (RR). Although additional gains in stored energy density is available with the integration of a flywheel into the modified RR of the machine, the power density decreases due to the addition of flywheel, and moreover, the constrain on size and difficulty of configuration fabrication and assembly make the scheme impracticable.

For achievement of excellent performance parameters, the chosen design topology of the air-core large-scale compulsator is based on a modified RR configuration.

As shown in Fig. 1, this topology uses a rotor core mounted on a metallic shaft by two hubcaps to support the rotating

Manuscript received December 21, 2009; revised March 10, 2010; accepted June 8, 2010. Date of publication August 3, 2010; date of current version January 7, 2011. This work was supported in part by the General Armament Department, through the Advanced Project, under Contract 51326020402.

Q. Zhang, S. Wu, S. Cui, and L. Song are with the Department of Electrical Engineering, Harbin Institute of Technology, Harbin 150001, China (e-mail: zhang_qianfan@hit.edu.cn; wushaopeng@hit.edu.cn; cuiism@hit.edu.cn; lw_song@hit.edu.cn).

C. Yu was with the Beijing Institute of Special Electromechanical Technology, Beijing 100012, China. He is now with the University of Science and Technology Beijing, Beijing 100083, China.

Color versions of one or more of the figures in this paper are available online at <http://ieeexplore.ieee.org>.

Digital Object Identifier 10.1109/TPS.2010.2053221

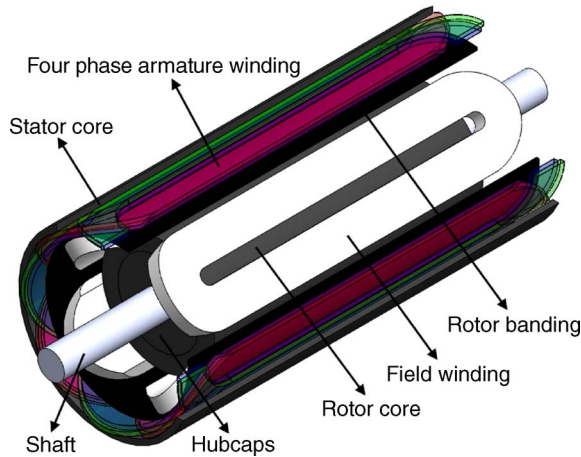


Fig. 1. Three-dimensional diagram of the designed model-scale compulsator.

armature. Rotor banding, made from high-strength carbon-fiber-enhanced epoxy composite banding, is used to limit the centrifugal radial growth of the field winding such that it remains in radial compression against the rotor structure throughout the operating speed range of the machine. The carbon-fiber-enhanced epoxy composite stator core supports the slotless armature windings and provides a torque path to ground. An even number of phase-nested armature windings are designed to increase the condition flexibility of the discharge-current shape and reduce the repulsive loads between armature phases during commutation by properly phase sequencing the windings during discharge.

III. EVALUATION OF ELECTROMAGNETIC FIELD

The electromagnetic-field design is used to evaluate the power generated. The capacity of the machine to generate the power required for the discharge must be matched with that required by the railgun. The finite-element analysis (FEA) electromagnetic-field simulation can be easily conducted with a commercial code.

Although the 3-D FEA simulation is closer to the practical prototype than the 2-D FEA simulation, the former will cost plenty of time due to the large size of the model-scale compulsator, which is unnecessary for the first-stage design. Therefore, the 2-D FEA simulation was used for electromagnetic-field evaluation as shown in Fig. 2.

In order to make predictions of applicability, the calculations and initial design processes should be expeditious and sometimes with reasonable expenses. The magnetic vector potential method is applied to axial symmetry electromagnetic-field calculation of the compulsator. The analytical solution of magnetic field was presented on the basis of some assumptions [8]. With the quick development and widespread application of commercial FEM codes, less time has been spent by supercomputers in running advanced software to solve the transient electromagnetic fields which occur in the discharging pulsed rotating generators. It can be compared with the FEM solution. The hybrid FE/BE method was applied to 2-D and 3-D symmetric electromagnetic-field calculations, including the stress and thermal coupling in EMAP3D code [9], [10]. The code was deduced from Maxwell formulation and stress and

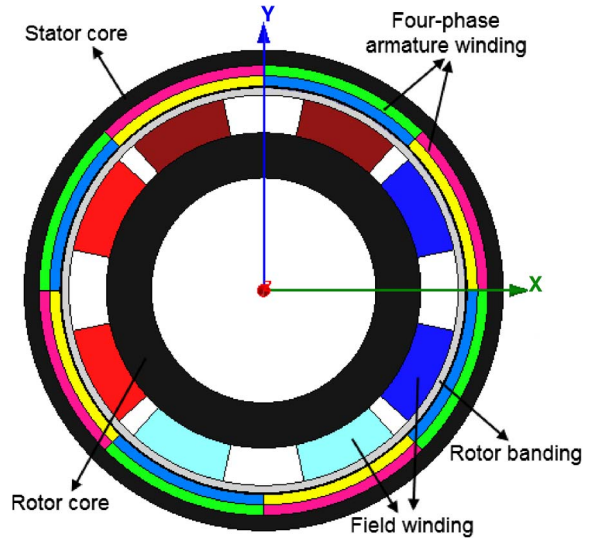


Fig. 2. Two-dimensional FEA model for electromagnetic-field simulation.

TABLE I
PARAMETERS OF THE DESIGNED MODEL-SCALE COMPULSATOR

Parameters	Value
Peak Discharge Current I_p	5 MA
Phase Voltage U_a	14 kV
Peak Power P_p	70 GW
Peak Excitation Current I_f	10 kA
Rotor Energy E_r	1200 MJ
Phases N_{ph}	4
Poles P	4
Maximum Speed n_0	20 000 rpm
Armature winding turns per pole N_A	4
Excitation coil turns per pole N_E	25
Rotor Outer Radius b_r	0.54 m
Rotor Inner Radius a_r	0.3 m
Rotor Length l_r	2 m
Compulsator Radius c_r	0.7 m
Compulsator Length c_l	2.25 m

TABLE II
INPUT PARAMETERS FOR SIZING THE RAILGUN LOAD

Parameters	Value
Muzzle Energy E_m	60 MJ
Muzzle Velocity V_m	4000 m/s
Peak Bore Pressure P_b	4×10^8 Pa
Piezometric Efficiency η_p	0.7
Gun Length l_g	6 m
Gun Inductance Gradient L'	4.8×10^{-7} H/m

thermal formulations, and mesh generation was achieved by a commercial FEM code, including several excellent algorithms. A good idea was shown in solving the special electromagnetic components.

The basic design parameters of the model-scale compulsator are shown in Table I.

The stored energy and power generated by the compulsator are related to the requirement of the railgun. Some important railgun parameters are given in Table II.

Piezometric launch efficiency is defined as the average launch acceleration divided by the peak launch acceleration and is important because it can significantly affect the peak-power demand on the compulsator. Likewise, a long gun length will result to a lower peak power required from the pulsed-power source for a given launch energy.

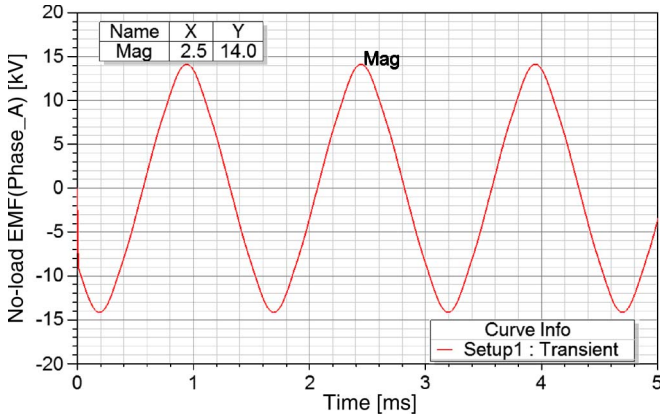


Fig. 3. No-load EMF of phase A at 10-kA excitation current and 20-000 rev/min speed.

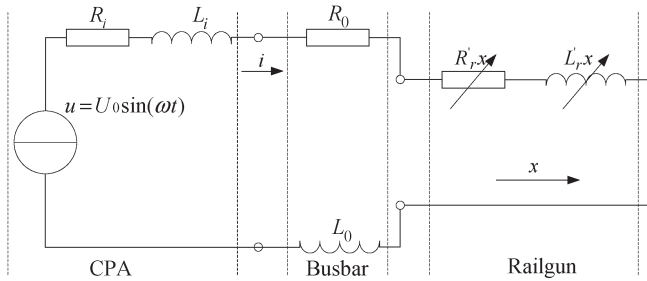


Fig. 4. Schematic circuit of CPA discharge into a railgun load.

The electromagnetic design is based on the 2-D FEA to some extent for achieving the relationship between rotating speed, excitation current, and magnitude of no-load back electromotive force (EMF) in a fixed size of a compulsator. The magnitude of the no-load EMF of the armature winding is 14 kV, as shown in Fig. 3, when the rotating speed is 20 000 rev/min, and the excitation current is 10 kA.

The electromagnetic field in the compulsator increased with the excitation current increasing in exponential during the self-excitation process until the final excitation current was reached, and end of the process was forced. To evaluate the ability of the compulsator quickly, the process is neglected in the first-stage design, and the final magnetic-flux density in the airgap is studied. Circuit simulation is needed to simulate the detailed process of self-excitation. The maximum final flux density is below 1 T, which could restrain electromagnetic interference of the compulsator with the control components. The air-core electromagnetic-field simulation results show a reasonable electromagnetic design.

The discharge schematic circuit of CPA as power supply for a railgun load is shown in Fig. 4. It consists of three parts: the CPA, busbar, and railgun load.

The control equations of the discharge process are based on

$$\frac{di}{dt} = \frac{U_0 \sin(\omega t) - i(R_i + R_0 + R'_r x + L'_r v_p)}{L_i + L_0 + L'_r x} \quad (1)$$

$$\frac{dx}{dt} = v_p \quad (2)$$

$$\frac{dv_p}{dt} = \frac{L'_r i^2}{2m} \quad (3)$$

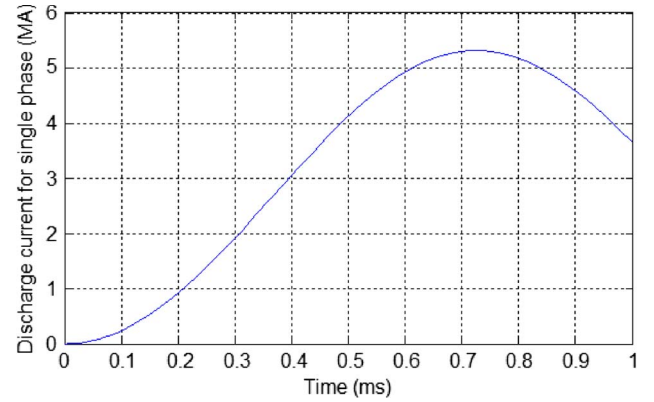


Fig. 5. Numerical discharge current for single phase.

where

- $u = U_0 \sin(\omega t)$ no-load voltage of CPA;
- R_i, L_i internal resistance and inductance of the CPA, respectively;
- R_0, L_0 resistance and inductance of busbar, respectively;
- R'_r, L'_r resistance gradient and inductance gradient of railgun, respectively;
- m sum of armature mass and projectile mass;
- v_p velocity of armature and projectile;
- i discharge current.

There are no analytical solutions for the aforementioned equations. The numerical solution of the discharge current for single-phase armature is shown in Fig. 5. In practical operation, the multiphase armatures will discharge the railgun load by commutation. The estimated maximum propulsive force of a projectile during discharge is 6.7 MN, as calculated by (3).

IV. PROCESS OF DESIGN

The first-stage design of the model-scale compulsator is based on the following analytical relationships. The performance of the compulsator can be on a first order as concluded from the following relationships.

A. Rotor Size

The compulsator integrates the rotor kinetic energy and stator electromechanical energy conversion into a unit. The main sizes of the compulsator have a direct impact on the energy storage and peak power. The rotor energy of the compulsator E_r can be concluded from

$$E_r = \frac{\pi}{4} \rho_{\text{avg}} \beta (1 - \lambda^4) b_r^3 v_{\text{tip}}^2 \quad (4)$$

where

- ρ_{avg} average density of rotor;
- β ratio of rotor length to radius;
- λ ratio of inner radius to outer radius;
- b_r outer radius of rotor;
- v_{tip} tip speed of rotor.

Each parameter has limits on the degree to which they can be adjusted to meet the energy-storage requirement.

The rotor consists of field winding made of aluminum Litz conductors, a shaft made of titanium, and other components

made from carbon-fiber-enhanced epoxy composite. In order to increase the energy and power densities, aluminum Litz conductors lighter than copper conductors are used to reduce the mass of the compulsator. The fraction of aluminum Litz conductors in the rotor is selected according to electromagnetic simulation. The average density of the rotor is affected by the fraction of aluminum Litz conductors. ρ_{avg} is equal to 2200 kg/m^3 for estimation here.

The following rules have been adopted to avoid generating-problem designs. The rotor length to radius ratio will be constrained to a maximum value of four to avoid lowering the rotor-bending vibration modes to unacceptably low levels. β is 3.7, which is within the reasonable range of 2–4. The rotor-radius ratio λ , which must be between 0.4 and 0.7 for practical designs, is 0.56.

The v_{tip} is limited by the hoop stress σ_{θ} of the rotor banding made up of composite material, according to (5). While this simple relationship does not account for the actual size of the rotor windings required for the system, it does provide an initial estimate of the required banding performance and allows the impact of improved banding materials to be explored. The v_{tip} is also limited if a mechanical bearing is used

$$\sigma_{\theta} = \rho_{\text{avg}} \bullet v_{\text{tip}}^2, \quad (5)$$

σ_{θ} is 2.8 GPa for the design, which is within the reasonable range of 0.9–3.8 GPa. There exists a carbon-fiber composite material whose longitudinal stress is 2.8 GPa.

B. Stator Size

In general, the stator includes two-thirds armature winding and one-third stator core, made up of carbon-fiber epoxy composite material. There are four-phase nested armature windings bonded in the cylindrical stator core. Four-phase windings are designed to increase the condition flexibility of the discharge current shape and reduce the repulsive loads between armature phases during commutation events. The turns of the winding are designed mainly by the maximum instantaneous single-phase voltage requirement for railgun load. There are five turns per coil of armature winding.

C. Energy-Density Evaluation

The energy density is a very important performance target in compulsator design, particularly as pulsed-power supply for land-based or air-based railgun system. The energy density of the rotor is shown as

$$E_r/m_r = F_s \bullet \sigma_{\theta \text{ max}}/\rho_{\text{eff}} \quad (6)$$

where

- F_s shape factor of the rotor defined in [11];
- $\sigma_{\theta \text{ max}}$ maximum-hoop stress strength of rotor material;
- ρ_{eff} effective mass density of rotor.

The shape factor of the rotor is calculated by (7) in which there is no radial stress in the composite material of the rotor

$$F_s = \frac{1}{4}(1 + \lambda^2). \quad (7)$$

TABLE III
STRESS/DENSITY RATIO COMPARISON OF SELECT ROTOR MATERIALS

Materials	Stress (MPa)	Density (kg/m ³)	Stress/Density
Steel	1724	7870	0.032
Titanium	1034	4540	0.033
Carbon fiber epoxy	3103	1770	0.254

The shape factor in the design is 0.33 lower than in laminated disk and RR configuration, which was designed by CEM researchers. If the shape factor increases, such as, if the inner radius of rotor increases, the energy density will increase, but the net kinetic energy will decrease. Radial stress had an impact on the shape factor [12]. With the rotor size fixed, several concentric layers of composite with multiple shrink fits were used to prestress the rotor at rest and that the stress profile was made uniform in speed to increase the shape factor. From (7), it is obvious that if the shape factor is fixed, the energy density is proportional to the ratio of the hoop-stress strength to the effective mass density. The ratio of the composite material, such as carbon-fiber epoxy composite, is higher than steel or titanium, as shown in Table III. If the energy density is a prior consideration in design, the carbon-fiber epoxy composite is the most excellent material.

D. Evaluation of Thermal Aspect

Although the instantaneous electrical loading of the compulsator is much larger than that of continuous duty electrical machine, a reasonable match of instantaneous electrical loading and pulse operation time of compulsator can make the Joule heat within a safe range for the winding dielectric material to withstand during the short discharge time. Due to the short time (milliseconds level), the heat energy of the armature winding conducted to its surrounding environment is negligible. The Joule heat is assumed to be thoroughly used to increase the temperature of the conductor. Therefore, the available area of the armature cross section can be concluded according to [13]

$$S \geq I_s \sqrt{\alpha \rho_0 T_k / \{c \gamma \ln [(1 + \alpha \theta_s)/(1 + \alpha \theta_0)]\}} \quad (8)$$

where

- I_s magnitude of single discharge current;
- T_k single discharge electrical period;
- α temperature coefficient of resistance;
- ρ_0 resistivity of winding conductors;
- θ_0 initial temperature before discharge;
- θ_s temperature after single discharge;
- c specific heat of winding conductors;
- γ mass density of winding conductors.

The aforementioned parameters for field winding and armature winding were inserted into (8), and two inequalities were satisfied. The safe factor for armature winding is above two. In actual combat, multiple compulsator discharge is almost needed for enhancing instantaneous fire. The evaluation of thermal aspects is based on the interval of pulse and cooling condition. Cooling structure should be designed for compulsator safe operation and long life span.

E. Evaluation of Structural Aspect

The exact forces, including electromagnetic force and mechanical force distribution, are based on the precise electromagnetic and structural coupling FEA. However, in the first-stage design, only the evaluation of the weakest part in the compulsator was presented, as in the following.

The lowest rotor-discharge speed will result in the highest discharge torque, so it should be used for this calculation. The estimation of discharge torque T during discharge is

$$T = P_p/\omega_f = \tau_{\text{avg}}Ab_r \quad (9)$$

where

- P_p peak power;
- ω_f final speed after discharge;
- τ_{avg} average shear stress of the armature;
- A shear armature area available to react to the discharge.

The shear armature area A available to react to the discharge torque is determined by the armature winding distribution

$$A = 2\pi b_r l_r / f_a \quad (10)$$

where

- $f_a = 1$ for stacked armature;
- $f_a = N_{\text{ph}}/2$ for nested armature.

The compulsator presented is a four-phase nested armature, so f_a is equal to two.

The final speed ω_f is related to the fraction of useable energy in the rotor, as shown in

$$\omega_f = \sqrt{1 - f_u} \omega_0 \quad (11)$$

where, f_u is the fraction of useable energy, as shown in (12).

The rotor energy for shooting is shown in

$$f_u = \Delta E_r / E_r \quad (12)$$

$$\Delta E_r = E_m / \eta_l \quad (13)$$

where η_l , assumed here to be 0.4, is the launch efficiency.

Based on experience, the compulsator must have about 50% more voltage than is required by the railgun to overcome the internal impedance of the compulsator and associated switching losses. According to the previous formulas, an estimate of the average shear stress that the armature winding will experience can then be obtained by increasing the railgun power required by 50% and solving (14) for τ_{avg}

$$\tau_{\text{avg}} = 1.5 P_p f_a / 2\pi b_r^2 l_r \omega_f. \quad (14)$$

The calculated average shear stress for the model-scale compulsator is 21 MPa, which is within the reasonable range of 6.9–27.6 MPa.

V. CONSIDERATION OF FABRICATION TECHNIQUE

The design and fabrication technique for some critical components for the model-scale compulsator are directly related to the feasibility of the whole design.

A. Composite-Material Component

The carbon fiber has very large stress in the longitudinal direction but small shear stress in the transverse direction. Take T700, for example, the ultimate stress in the longitudinal direction is 2500 MPa, but the stress is only 20 MPa in the transverse direction.

The hoop stress and radial stress in single-hoop-winding composite layer due to the centrifugal force in high rotating speed is shown in (15) and (16), respectively [14], i.e.,

$$\sigma_\theta = \rho_{\text{eff}} v_0^2 \frac{3+v}{9-\mu^2} \left[\mu l \left(\frac{r}{r_o} \right)^{\mu-1} + \mu(l-1) \left(\frac{r}{r_o} \right)^{-\mu-1} - \frac{\mu^2 + 3v}{3+v} \left(\frac{r}{r_o} \right)^2 \right] \quad (15)$$

$$\sigma_r = \rho_{\text{eff}} v_0^2 \frac{3+v}{9-\mu^2} \times \left[l \left(\frac{r}{r_o} \right)^{\mu-1} - (l-1) \left(\frac{r}{r_o} \right)^{-\mu-1} - \left(\frac{r}{r_o} \right)^2 \right] \quad (16)$$

where

$$l = (\lambda^{-\mu-1} - \lambda^2) / (\lambda^{-\mu-1} - \lambda^{\mu-1});$$

$\mu = \sqrt{E_\theta/E_r}$ a parameter presenting the anisotropic degree of material;

ν Poission ratio of fiber.

The stress distribution in the hoop and radial directions is determined by the value of μ . The value of μ can be optimized by the modulus of the fiber and epoxy and the volume occupied by fraction of the fiber and matrix in the composite ring, as shown in

$$E_\theta = E_f V_f + E_m V_m \quad (17)$$

$$E_r = E_f E_m / (V_m E_f + V_f E_m) \quad (18)$$

where

E_f, E_m elastic moduli of fiber and matrix, respectively;

V_f, V_m volume occupied by fraction of fiber and matrix.

Although from (16)–(18), the radial stress can be decreased in some degree, the single composite layer tends to delamination failure in high speed.

There are several methods to decrease the radial stress in the rotor. Multirings are assembled by interference fit. The composite part of the rotor is made up of several concentric layers, which have multiple shrink fit at rest, to compensate the radial stress due to centrifugal load at normal speed. The layer is wound according to radial interlayer thickness, laying angle of the fiber, and excess value of fiber interlayers. There are different laying angles of the carbon fiber for obtaining reasonable structure size and optimized energy density. The radial stress in the multiring is lower than that in the single-ring, at the same rotating speed and anisotropic degree of material, as shown in Fig. 6. The solid curves represent the three rings of the composite, and the dotted curves represent the single ring of the composite. The distribution of radial stress in the multiring is much more uniform than that in the single ring. The shape factor also increases in the multiring configuration.

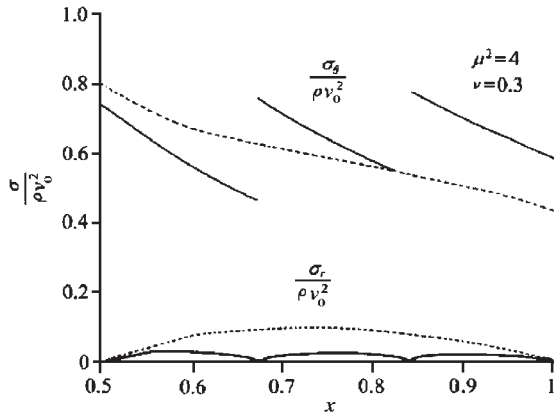


Fig. 6. Comparison of stress distribution between single ring and multiring.

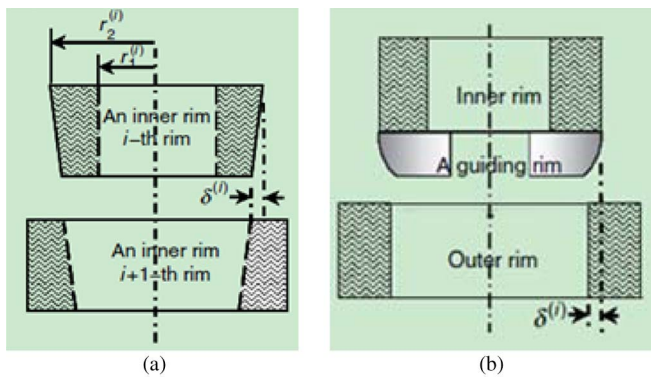


Fig. 7. Mechanical methods of press fitting the inner rim to outer rim. (a) Tapered rim. (b) Guiding rim.

In order to reduce the mass of the rotor, the rotor endplates are also made of carbon-fiber epoxy composite material, where the RTM technique is used for complex-shaped composite structure.

B. Rotor-Composite Assembly

The multirings were assembled together by press-fit interferences for suppressing the centrifugal force. In the assembly of press-fit interferences for the metal rings, the inner rim or outer rim is usually assembled by thermal heating or cooling and pressed into the outer rim quickly, as what the CEM scholar did in the composite rotor of RD configuration. However, most composite materials show very low thermal expansion, which is insufficient for the required press fitting [15]. Carbon-fiber composites show almost zero thermal expansion; hence, other methods of press fitting the composite materials are needed.

Generally, there are physical and mechanical methods to realize interference fit assembly. The mechanical methods are shown in Fig. 7.

The final assembly method is determined by situation and equipment.

C. Slotless Winding

It is unnecessary to machine slots in the fiber epoxy composite for preventing cutting the fiber. Slotless winding is used in air-core compulsator. The conductors are covered with some

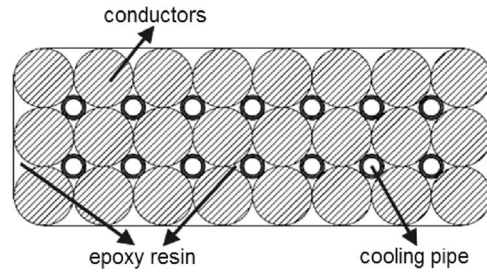


Fig. 8. Placement of conductors and cooling pipe.

new type of insulation materials. From thermal simulation of the air-core compulsator, it can be concluded that the cooling system must be designed for air-core compulsator due to the high heat produced in the windings and low heat-release coefficient of epoxy and composite support structure.

The fabrication and shape technique of slotless winding are very important in the design of compulsator. The forming of slotless winding consists of two processes: preforming and final shape in mould. The conductors, cooling pipes, and glass-fiber epoxy-enhanced material filling in the spacing between conductors and pipes are first laid, as shown in Fig. 8.

The conductors and cooling pipe are laid in a final-shape module and fabricated according to the inner and outer radius size. Then, modified epoxy with higher strength is filled into the intervals between the conductors and cooling pipe. Then, it is heated in a furnace for curing, with an insulation cloth covering the outside of the whole coil. In addition to enhancing the mechanical strength and ensuring the size, the epoxy also enhances the turn-to-turn insulation. The insulation cloth was used to enhance the insulation of coil and carbon-fiber epoxy stator core.

VI. SELECTION OF AUXILIARY

The development of the compulsator is, to a great extent, matched with the development of the materials in critical auxiliary component.

A. Bearing

Although the mechanical bearing can withstand the compulsator-rotor rotation at 20 000 rev/min with the use of lubricating oil, the system configuration and control are complex. Due to the high rotating speed of the compulsator, the mechanical rolling element of the bearing cannot stand the large loss, the life span decreases, and the maintenance cost increases. Although the magnetic suspension bearing can be selected for high speed and easy control and frictionless, the control is difficult, and real-time speed and precision feedback control are highly required. The strong discharge field may affect the magnetic suspension bearing, and it needs further exploration. The quantitative representation the reliability of mechanical rolling element bearing is higher than active magnetic bearing (AMB) in any scenario where controller input power is lost, including human errors introduced by improper shutdown sequence or failures [16]. The high-temperature superconducting levitation can fulfill self-stable nature where other levitations cannot. The friction coefficient of the high-temperature superconducting

magnetic bearing (HTSMB) is 10^{-7} , which is 1/1000 of AMB and 1/10 000 of the best mechanical bearing [17], [18]. The HTSMB system has advantages, like high efficiency, longevity of service, and low maintenance. The only problem is the need for cryogenic cooling systems. If high-temperature superconductors are used in the manufacture of field and armature windings, the cryogenic cooling systems can be used for the field winding, armature windings, and HTSMB system at the same time.

B. Brush Slip-Ring Mechanism

The model-scale compulsator needs high rotating speed and high-power brush slip-ring mechanism. Since the excitation current is at a large level, multiple brush columns along the circumferential direction per slip ring channel are used for reducing the current flowing in a single brush. Due to high rotating speed and high power, the operating environment for the brush slip-ring mechanism as current collector becomes worse and worse. Several problems can occur, such as overheating of slip ring and brushes, sparking, and conductor burning or blowing. This is because the electric current is not evenly distributed to the parallel brush while the brush is used for high-power generator and high-speed slip rings. These problems are resolved when a brush with many pores is used. Brushes with high open porosity and low volume density should be chosen [19].

VII. CONCLUSION

Through the first-stage design, the main parameters of a model-scale compulsator based on a railgun launch system have been presented. The first-stage electromagnetic, structural, and thermal evaluation accuracy, to some extent, had been done for achieving a safe and reasonable design scheme quickly. Energy storage and power density of 191 J/g and 8.2 kW/g, respectively, were achieved based on the designs explored in this paper. Critical design and fabrication techniques of the components were discussed. However, a lot of detailed simulation works, such as motoring, thermal management, energy recovery, torque reaction, and controls, should be considered during the next step.

REFERENCES

- [1] M. L. Spann, W. L. Bird, W. F. Weldon, and H. H. Woodson, "The design, assembly, and testing of an active rotary flux compressor," in *Proc. 3rd IEEE Int. Pulse Power Conf.*, Albuquerque, NM, Jun. 1–3, 1981, pp. 300–303.
- [2] M. D. Werst, D. E. Perkins, S. B. Pratap, M. L. Spann, and R. F. Thelen, "Testing of a rapid fire, compensated pulsed alternator system," *IEEE Trans. Magn.*, vol. 25, no. 1, pp. 599–604, Jan. 1989.
- [3] J. R. Kitzmiller, R. W. Faidley, R. N. Headifen, R. L. Fuller, and R. F. Thelen, "Manufacturing and testing of an air-core compulsator driven 0.60 caliber railgun system," *IEEE Trans. Magn.*, vol. 29, no. 1, pp. 441–446, Jan. 1993.
- [4] W. A. Walls, S. B. Pratap, W. G. Brinkman, K. G. Cook, J. D. Herbst, S. M. Manifold, B. M. Rech, R. F. Thelen, and R. C. Thompson, "A field based, self-excited compulsator power supply for a 9 MJ railgun demonstrator," *IEEE Trans. Magn.*, vol. 27, no. 1, pp. 335–340, Jan. 1991.
- [5] J. R. Kitzmiller, S. B. Pratap, M. D. Werst, C. E. Penney, T. J. Hotz, and B. T. Murphy, "Laboratory testing of the pulse power system for the cannon caliber electromagnetic gun system (CEMAG)," *IEEE Trans. Magn.*, vol. 33, no. 1, pp. 443–448, Jan. 1997.
- [6] J. R. Kitzmiller, S. B. Pratap, and M. D. Driga, "An application guide for compulsators," *IEEE Trans. Magn.*, vol. 39, no. 1, pp. 285–288, Jan. 2003.

- [7] W. A. Walls, "Advanced compulsator topologies and technologies," Ph.D. dissertation, Univ. Texas Austin, Austin, May 2002.
- [8] S. J. Oh, "Electromagnetics of inertial energy storage systems with fast electromechanical energy conversion," Ph.D. dissertation, Univ. Texas Austin, Austin, May 2000.
- [9] V. Thiagarajan and K.-T. Hsieh, "Investigation of a three dimensional hybrid finite element/boundary element method for electromagnetic launch applications and validation using semi-analytical solutions," in *Proc. 12th EML Symp.*, May 25–28, 2004, pp. 375–380.
- [10] V. Thiagarajan and K.-T. Hsieh, "Computation of magnetic fields using a 2-D hybrid finite-element/boundary-element algorithm and comparison with analytical solutions," *IEEE Trans. Magn.*, vol. 41, pt. 2, no. 1, pp. 393–397, Jan. 2005.
- [11] R. Acebal, "Shape factors for rotating machines," *IEEE Trans. Magn.*, vol. 33, no. 1, pp. 753–762, Jan. 1997.
- [12] R. Acebal, "Effect of shape factor, operating stresses, and electrical conductors on the energy density of rotating machines," *IEEE Trans. Magn.*, vol. 32, no. 2, pp. 421–425, Mar. 1996.
- [13] K. Zheng, "Research of permanent passive compulsator," M.S. thesis, Huazhong Univ. Sci. Technol., Wuhan, China, Apr., 2004.
- [14] S. K. Ha and H. H. Han, "Design and manufacture of a composite flywheel press-fit multi-rim rotor," *Int. J. Mech. Sci.*, vol. 43, no. 4, pp. 993–1007, 2001.
- [15] S. K. Ha and H. T. Kim, "Measurement and prediction of process-induced residual strains in thick wound composites rings," *J. Composite Mater.*, vol. 37, no. 14, pp. 1223–1237, 2003.
- [16] Quantitative Reliability Assessment of Ball Bearings Versus Active Magnetic Bearings for Flywheel Energy Storage Systems, white paper 111 of Active Power corporation.
- [17] J. R. Hull, "Superconducting bearings," *Supercond. Sci. Technol.*, vol. 13, no. 2, pp. R1–R15, Feb. 2000.
- [18] K. B. Ma, Y. V. Postrekhin, and W. K. Chu, "Superconductor and magnet levitation devices," *Rev. Sci. Instrum.*, vol. 74, no. 12, pp. 4989–5017, Dec. 2003.
- [19] Z.-W. Feng, K.-X. Zhang, and S.-L. Liang, "Simple study of brush for generator high speed slip-rings," *Carbon*, no. 2, pp. 23–25, 2000.



Qianfan Zhang was born in Heilongjiang province, China, on September 13, 1974. He received the B.S. and Ph.D. degrees in electrical engineering from the Harbin Institute of Technology (HIT), Harbin, in 1999 and 2004, respectively.

Since 1999, he has been with the Department of Electrical Engineering, HIT, where he was a Faculty Member and has been an Associate Professor since 2005. From 2006 to 2007, he was a Postdoctoral Researcher with the National University of Ireland, Galway, Ireland. His research interest includes

electric-machine drives, power electronics, electric system on EV and HEV, and photovoltaic applications.

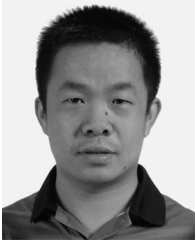


Shaopeng Wu (S'10) was born in Heilongjiang Province, China, on July 1, 1983. He received the B.S. degree in electrical engineering from the Harbin Institute of Technology, Harbin, China, in 2005, where he has been working toward the combined M.S.–Ph.D. degree program in the Institute of Electromagnetic and Electronic Technology, since September 2005.

He specializes in the research field of compulsator, including the analysis of electromagnetic field and structural stress field, and the design and fabrication

of prototypes.

Mr. Wu is a Student Member of the IEEE Magnetics Society and the IEEE Nuclear and Plasma Sciences Society in 2010. He has several papers published in the IEEE TRANSACTIONS ON MAGNETICS and the IEEE TRANSACTIONS ON PLASMA SCIENCE. He was the recipient of the Peter J. Kemmeyer Memorial Scholarship by the 15th International EML Symposium, Brussels, Belgium, in 2010.



Chengda Yu was born in Shandong province, China, on November 27, 1976. He received the B.S. degree in electrical engineering from the Naval University of Engineering, Wuhan, China, in 2003. He is currently working toward the Ph.D. degree in weapons science and technology at the University of Science and Technology Beijing, Beijing, China.

He was with the Beijing Institute of Special Electromechanical Technology, Beijing, from 2003 to 2007. His research interests focus on pulsed-power source technology in the field of electromagnetic

launch.



Shumei Cui was born in Heilongjiang province, China, on November 22, 1964. She received the Ph.D. degree in electrical engineering from the Harbin Institute of Technology (HIT), Harbin, China, in 1998.

She has been with HIT where she is a Professor in the Department of Electrical Engineering, the Vice Dean of the Institute of Electromagnetic and Electronic Technology, and the Dean of the Electric Vehicle Research Centre. Her research interests focus on design and control of micro and special electric machines, electric-drive system of electric vehicles, control and simulation of hybrid electric vehicles, and intelligent test and fault diagnostics of electric machines.

Prof. Cui serves as a vice director member of Micro and Special Electric Machine Committee, Chinese Institute of Electronics, and a member of the Electric Vehicle Committee, National Automotive Standardization Technical Committee.



Liwei Song was born in Heilongjiang province, China, on October 23, 1970. He received the B.S., M.S., and Ph.D. degrees in electrical engineering from the Harbin Institute of Technology (HIT), Harbin, China, in 1992, 1998, and 2004, respectively.

He has been a Professor with the Department of Electrical Engineering, HIT. His research interests focus on design and control of electric machines and research of electric machine with high power density and special structure.

Dr. Song was the recipient of the second prize of the National Tech & Invention Award, China, in 2006.